Electric-field-induced orthorhombic to rhombohedral phase transition in $[111]_C$-oriented $0.92Pb(Zn_{1/3}Nb_{2/3})O_3 - 0.08PbTiO_3$

Matthew Davis, Dragan Damjanovic, and Nava Setter

Citation: Journal of Applied Physics **97**, 064101 (2005); doi: 10.1063/1.1850181

View online: https://doi.org/10.1063/1.1850181

View Table of Contents: http://aip.scitation.org/toc/jap/97/6

Published by the American Institute of Physics

Electric-field-induced orthorhombic to rhombohedral phase transition in $[111]_C$-oriented $0.92Pb(Zn_{1/3}Nb_{2/3})O_3-0.08PbTiO_3$

Matthew Davis,[a] Dragan Damjanovic, and Nava Setter
Ceramics Laboratory, Ecole Polytechnique Fédérale de Lausanne (EPFL), Switzerland

(Received 9 August 2004; accepted 21 November 2004; published online 1 March 2005)

Strain-field measurements and *in situ* polarized light microscopy have been used to evidence a hysteretic, irreversible electric-field-induced transition to a quasimonodomain rhombohedral phase in $[111]_C$-oriented, pseudo-orthorhombic PZN−8PT $[0.92Pb(Zn_{1/3}Nb_{2/3})O_3-0.08PbTiO_3]$. This first-order transition most likely occurs following the simplest path O-M_B-R, i.e., via polarization rotation in the $(10\text{-}1)_C$ plane. The measured strain-field loops are compared to those for rhombohedral, $[111]_C$-oriented PMN−28PT $[0.72Pb(Mg_{1/3}Nb_{2/3})O_3-0.28PbTiO_3]$ and PMN −33PT $[0.67Pb(Mg_{1/3}Nb_{2/3})O_3-0.33PbTiO_3]$ where no electric-field-induced transition is possible. © *2005 American Institute of Physics*. [DOI: 10.1063/1.1850181]

I. INTRODUCTION

Relaxor-based ferroelectric single crystals, especially PMN−xPT$[(1-x)Pb(Mg_{1/3}Nb_{2/3})O_3-xPbTiO_3]$ and PZN −xPT$[(1-x)Pb(Zn_{1/3}Nb_{2/3})O_3-xPbTiO_3]$, continue to attract much attention. Rhombohedral crystals of either material oriented and poled along the $[001]_C$ prototypic cubic direction exhibit attractive, anhysteretic stress-field behaviors, and "giant" piezoelectric strain coefficients $d_{33}>2000$ pm/V.[1] Such converse piezoelectric properties make PZN−xPT and PMN−xPT very promising for next generation actuator technology.[2]

Separating the low $PbTiO_3$ content rhombohedral (R) phase and the high $PbTiO_3$ content tetragonal (T) phase in these materials is a partition region, the morphotropic phase boundary (MPB), occurring at around $0.08<x<0.09$ for PZN−xPT and $0.30<x<0.37$ for PMN−xPT.[3,4] High-resolution diffraction experiments[5–7] and even more recent dielectric studies,[8,9] polarized light microscopy,[10] and pyroelectric measurements[11] have confirmed the presence of a third phase existing at the MPB, of either orthorhombic (O, point-group $mm2$) or lower monoclinic symmetry (point-group m). In the latter monoclinic phase, denoted M_C by Vanderbilt and Cohen[12] and having orthorhombic limiting symmetry, the polarization vector is constrained to lie in the $(010)_C$ plane of the unit cell.

Since the presence of domains (or the controlled "domain-engineered" structure) plays only a partial role in the large d_{33} coefficients of $[001]_C$-oriented rhombohedral PMN−xPT and PZN−xPT,[13,14] efforts to understand their properties have concentrated on *intrinsic* effects, particularly as related to the monoclinic phases. The main approach has been aimed at the "polarization rotation mechanism" whereas a second strategy has been to consider more explicitly the large crystal anisotropy. In the former, based mainly on first-principles calculations,[15,16] the large piezoelectric coefficient is a consequence of the *rotation* (rather than the extension) of the polarization vector upon application of the off-axis field and, moreover, its relative ease in the presence of a monoclinic phase. In the latter phenomenological approach, dielectric, stiffness, and piezoelectric coefficients for the various crystallographic phases in $BaTiO_3$,[17,18] $PbTiO_3$,[18] and lead zirconate titanate[19] (PZT) have been calculated as a function of temperature and orientation. It has been shown that close to ferroelectric–ferroelectric phase transitions, piezoelectric shear coefficients can become very large.[18] Because this is, in itself, driven by augmentations of the transverse dielectric permittivity, it agrees well with the concept of easy polarization rotation. In most perovskites the d_{15} piezoelectric shear coefficient is the main component of the giant d_{33} value as measured in the $[001]_C$ direction.[2,13,18]

Most importantly, both approaches are inherently linked with the concept of phase transitions, whether induced by small changes in composition close to the MPB, by temperature or by an applied electric field. The electric-field-induced transition is nothing new; when an electric field E is applied along a certain crystallographic direction of a perfect crystal, at a sufficiently high field the phase with its polarization vector P along that direction will be favored due to the competitive $-PE$ term in the free-energy expansion.[20]

Various authors have used *in situ* diffraction, polarized light microscopy (PLM), and *ab initio* modeling to study field-induced phase transitions in these materials and their accompanying *polarization rotation path*. In $[001]_C$-oriented rhombohedral PZN−4.5PT, far away from the MPB, the transition sequence follows the path R-M_A-T, where the polarization rotates in the $(1\text{-}10)_C$ mirror plane of a second monoclinic phase (M_A).[5] As evidenced by *in situ* measurements of the lattice constants[5] and the hysteric strain-field loops,[21,22] the rotation is not continuous; there is a first-order jump in the polarization from M_A to T at a certain field value, whereas the initial R-M_A transition is reversible. In contrast PZN−8PT retains a "pseudo-orthorhombic" M_C symmetry after poling.[6] Here, subsequent application of a field along the $[001]_C$ direction leads to the simplest polarization rotation, M_C-T, in the $(010)_C$ plane. However, as for the PZN −4.5PT, the polarization rotation is initially reversible (and anhysteretic) until a hysteretic strain-field loop at higher

[a]Electronic mail: matthew.davis@epfl.ch

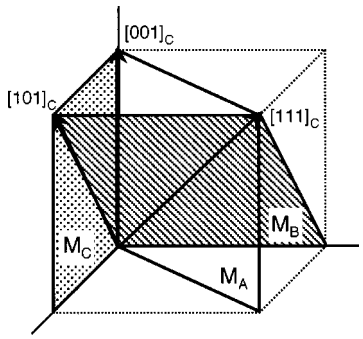

FIG. 1. Schematic drawing of the respective $[111]_C$, $[101]_C$, and $[001]_C$ polarization directions for the rhombohedral, orthorhombic, and tetragonal phases; also shown are the monoclinic planes $(1\text{-}10)_C$, $(10\text{-}1)_C$, and $(010)_C$ of the M_A,M_B, and M_C phases, respectively.

fields indicates a discontinuous jump of the polarization vector. The mirror planes for the M_A and M_C phases, and the polarization vectors for the limiting rhombohedral, orthorhombic, and tetragonal phases are shown in Fig. 1.

More interestingly, Viehland and Li have also reported a field-induced transition to an *orthorhombic* phase in $[101]_C$-oriented, rhombohedral PMN−30PT;[23] here, an anhysteretic strain-field loop suggests a completely reversible *T*-M_B-*O* transition via rotation in the $(10\text{-}1)_C$ plane. Furthermore, it has been shown that in an otherwise orthorhombic crystal of PZN−8PT oriented along the $[111]_C$ direction, a rhombohedral phase can be irreversibly induced by poling the sample at high fields and at subzero temperatures.[11] The question remains, therefore, whether or not this rhombohedral phase can be induced, reversibly or otherwise, by the application of an electric field alone.

This paper will present observations, by polarized light microscopy and high-field strain measurements, of an electric-field-induced orthorhombic to rhombohedral phase transition in a $[111]_C$-oriented orthorhombic sample of the PZN−8PT at room temperature. The converse piezoelectric response will be compared to that in rhombohedral PMN−33PT and PMN−28PT where no electric-field-induced phase transition can occur. The results will reiterate the universality of the electric-field-induced phase transition, especially in relaxor-ferroelectric single crystals close to the MPB where the threshold fields for the transitions are small.

II. EXPERIMENTAL METHOD

$[111]_C$-oriented samples of PMN−28PT and PMN−33PT, and PZN−8PT were acquired from HC Materials (Urbana, IL) and Microfine Technologies (Singapore), respectively. The as-received $10\times10\times0.5$ mm^3 plates were first cut into smaller pieces with an area of 5×5 mm^2. Two as-cut samples of each composition were then sputtered with gold electrodes. The two remaining samples were further ground and diamond polished to thicknesses above 200 μm and subsequently annealed for 5 h at 450 °C to alleviate any residual stresses. After the heat treatment, Laue diffraction was used to ensure that the surface was aligned to within ±0.5° and to identify the two $[-110]_C$ and $[-1\text{-}12]_C$ directions in the plane of the sample. Transparent indium tin oxide (ITO) electrodes were then applied to the polished crystals

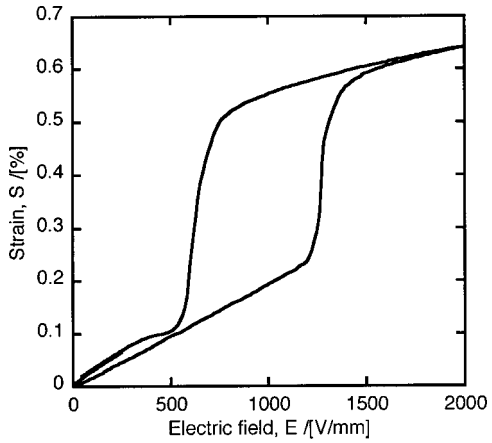

FIG. 2. Typical strain-field (*S*-*E*) loop for a $[001]_C$-oriented sample of PZN−8PT showing continuous rotation of the polarization within the $(010)_C$ plane of the monoclinic M_C phase before a hysteretic, discontinuous jump to the high-field tetragonal phase. The loop was measured using a LVDT system at a quasistatic frequency of 0.1 Hz.

by dc sputtering. A similar plate sample of $[001]_C$-oriented PZN−8PT (also from Microfine Technologies) was sputtered with gold for comparative strain-field measurements.

All crystals were poled by application of a low field (200 V/mm) upon cooling from the cubic phase to room temperature; we refer to this poling protocol as high-temperature field cooling (HTFC). This procedure ensures that a pseudo-orthorhombic (M_C or *O*) phase is stabilized in the PZN−8PT samples whereas the PMN−28PT and PMN−33PT samples are both "pseudorhombohedral" (*R* or M_A).[11] Measurements of permittivity were made using an impedance analyzer (HP 4194) at 1 kHz and room temperature, or upon heating at 2 °C/min to the paraelectric phase. Pyroelectric coefficients were measured using the dynamic method described well in Ref. 24 at a temperature of 25.5±0.5 °C. Converse piezoelectric (strain-field) measurements were made either using a linear variable differential transformer (LVDT), driven by a lock-in amplifier, or by a fiber-optic system (MTI-2000 Fotonic sensor) upon application of a unipolar sinusoidal field at low frequency (0.1 Hz). Optical micrographs were taken in transmission mode with the sample between crossed polarizers and the $[111]_C$ crystal axis parallel to the beam direction. The ITO covered samples were mounted on a rotating stage and high voltage was applied via copper wires attached with silver paste.

III. RESULTS AND DISCUSSION

The strain-field (*S*-*E*) loop measured for a $[001]_C$-oriented sample of the PZN−8PT using a maximum electric field of 2000 V/mm is shown in Fig. 2. As observed elsewhere,[6,25] the response is anhysteretic and linear before a large jump in a strain at a critical threshold field, $E_T \sim 1200$ V/mm. There is a good qualitative agreement between this *S*-*E* loop and the *in situ* lattice constants measured by Ohwada *et al.*[6] Explicitly, at zero field the sample is pseudo-orthorhombic having either *O* or (slightly distorted) M_C symmetry. As the field is increased the polarization rotates continuously and reversibly in the $(010)_C$ mirror plane of the monoclinic phase before jumping, irreversibly to a

TABLE I. Dielectric constants, loss tangents, and pyroelectric coefficients for $[111]_C$-oriented samples of PMN−33PT, PMN−28PT, and PZN−8PT. Values are given for the samples in the as-annealed (virgin) state, after field cooling (poling) from the Curie temperature under 200 V/mm, after unipolar (strain-field) cycling at fields <1000 V/mm, and finally, after cycling at larger fields (<2000 V/mm). Also given are the mean and standard deviations for two adjacent samples cut from the same piece and treated identically.

Composition	State	Dielectric constant, ε_{33}	Loss tangent, tan δ	Pyroelectric coefficient, $p/[\mu C\ m^{-2}\ K^{-1}]$
PMN−33PT	Virgin	3030±710	0.041	
PMN−33PT	Poled	910±120	0.017	951±34
PMN−33PT	$E<1000$ V/mm	720±10	0.008	
PMN−33PT	$E<2000$ V/mm	680±90	0.006	
PMN−28PT	Virgin	2730±40	0.047	
PMN−28PT	Poled	870±200	0.020	897±68
PMN−28PT	$E<1000$ V/mm	630±60	0.008	
PMN−28PT	$E<2000$ V/mm	560±100	0.005	
PZN−8PT	Virgin	4010±1300	0.037	
PZN−8PT	Poled	5600±230	0.023	614±21
PZN−8PT	$E<1000$ V/mm	4470±800	0.020	

high-field, monodomain tetragonal state at E_T. On decreasing the field, the metastable tetragonal phase is retained until a second discontinuous jump, still within the $(010)_C$ plane, back to the M_C phase. The gradient of the curve during the initial, continuous polarization rotation corresponds to a d_{33} of ~2000 pm/V. In contrast, the gradient corresponding to the collinear extension of the polarization vector in the tetragonal phase is ~670 pm/V.

The permittivities ε_{33}, dielectric loss tangents tan δ, and pyroelectric coefficients p for the $[111]_C$-oriented samples are given in Table I. In each case the two values from the pair of electroded samples were averaged. The standard deviations listed give an idea of the variation of properties in these crystals.

For both the PMN−28PT and PMN−33PT the permittivity drops significantly upon poling, in each case to below 1000, indicating a quasimonodomain "1*R*" rhombohedral state. The high pyroelectric coefficients also indicate a spontaneous polarization direction along the $[111]_C$ axis.[11] Moreover, the loss tangents, high compared to those for the $[001]_C$-oriented rhombohedral samples (<0.01), indicate the presence of a residual domain structure and the difficulty in stabilizing the 1*R* monodomain state in PMN−*x*PT discussed elsewhere.[26] In the PZN−8PT, however, the dielectric constant is higher in the poled sample indicating a polydomain, nominally 3*O*, pseudo-orthorhombic state.[11] Here, a slightly distorted orthorhombic phase, actually a M_B monoclinic phase[12] with its polarization direction constrained to lie in the $(10\text{-}1)_C$ plane (Fig. 1), might equally be irreversibly "locked in" during the $[111]_C$ poling regime.

Figure 3 shows strain-field loops for samples of the PMN−33PT and PMN−28PT immediately after HTFC poling and upon unipolar cycling at electric fields $E<1000$ V/mm. The responses are hysteretic, demonstrating significant domain reorientation toward the monodomain 1*R* state with a coercive field for switching of ~100 V/mm. The behavior is very similar to that observed in the $[111]_C$-oriented rhombohedral PZN−4.5PT by Liu *et al.*[21] After repeated cycling, the dielectric constant and the loss tangent were reduced in both the PMN−28PT and PMN−33PT, indicating that the samples became better poled (Table I).

Figure 4 shows the strain-field behavior of the same sample of PMN−33PT after repeated strain-field cycling at peak electric fields $E<2000$ V/mm. The reduced strain response, compared to that in Fig. 3, is evidence of further irreversible domain switching (or better poling) during the high-field cycling, and therefore a lower extrinsic contribution to the piezoelectric response. Accordingly, the loss tangents and dielectric constants in the PMN−33PT and PMN−28PT samples were again reduced, as shown in Table I. Finally, at the highest fields, the unstable 1*R* monodomain state is approached and the corresponding gradient of the strain-field loop gives a d_{33} value of ~110 pm/V. This is similar to the corresponding value of ~125 pm/V reported for rhombohedral PZN−4.5PT.[21]

Figure 5 shows the strain-field loop for an ITO-electroded, psuedo-orthorhombic sample of the PZN−8PT for peak fields <1400 V/mm. The differing behaviors be-

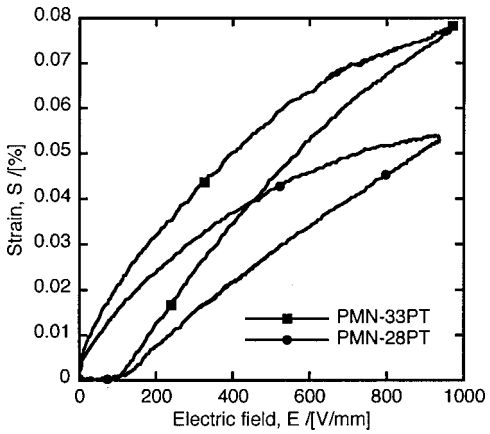

FIG. 3. Strain-field loops for $[111]_C$-oriented samples of PMN−33PT and PMN−28PT, immediately after poling and upon unipolar cycling at electric fields $E<1000$ V/mm. The loops were measured using a LVDT system at low frequency (0.1 Hz).

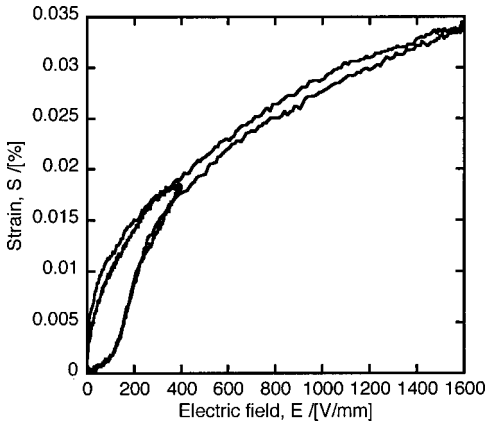

FIG. 4. Strain-field loops for the same $[111]_C$-oriented sample of PMN−33PT measured in Fig. 3. Two loops are shown, both taken after repeated cycling at high fields $E<2000$ V/mm and at a frequency of 0.1 Hz, at two differing peak fields.

tween the rhombohedral PMN−xPT samples and the PZN−8PT sample are obvious; most significantly, the PZN−8PT sample demonstrates a hysteretic jump in strain, characteristic of a first-order, field-induced phase transition. As is the case for the $[001]_C$-oriented PZN−8PT (Fig. 2), the response at low fields is quasilinear and anhysteretic with a d_{33} of 430 pm/V here, calculated from the gradient of the initial, linear portion of the loop. Subsequently, at a threshold field E_T of ~400 V/mm, there is large, vertical jump indicative of a phase transition. This is followed, finally, by hysteretic behavior at higher fields resembling that of the PMN−28PT and PMN−33PT, where there is domain reorientation towards the monodomain 1R rhombohedral state.

Polarized light microscopy was used to confirm the presence of a high-field rhombohedral phase. Figure 6 shows a series of optical micrographs taken through crossed polarizers, upon *in situ* application of an electric field to the same sample of the PZN−8PT. In this technique, most information about crystal structure can be attained by looking for directions of "extinction"; a good description of this is given in Ref. 27.

Under zero field, with the sample edges parallel to the

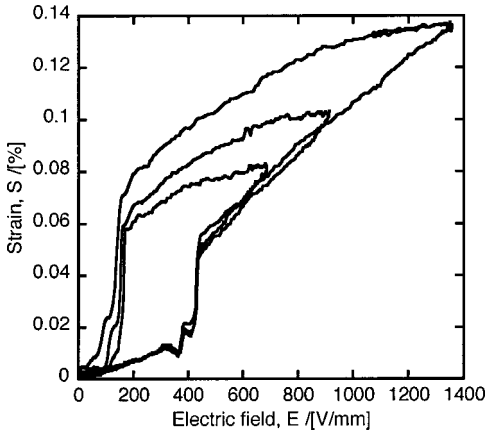

FIG. 5. Strain-field loop for a $[111]_C$-oriented pseudo-orthorhombic sample of PZN−8PT. The loop was taken using a LVDT system at room temperature upon application of a unipolar electric field at 0.1 Hz. A hysteretic, electric-field-induced phase transition is evident.

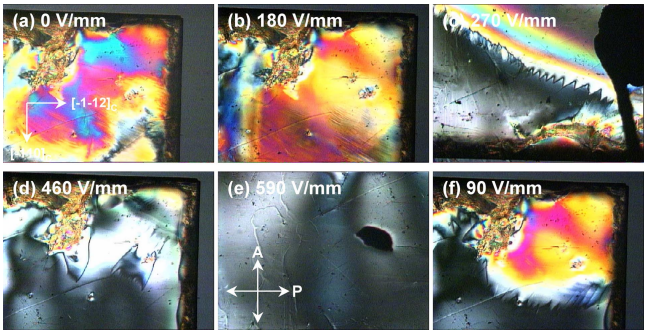

FIG. 6. (Color online) Polarized light micrographs taken *in situ* of the electric-field-induced phase transition from a pseudo-orthorhombic to a rhombohedral phase on application of a field along the $[111]_C$ direction in PZN−8PT. Micrographs at zero field (a), increasing field [(b)–(e)], and decreasing field (f) are shown, where the field was ramped up and down manually in steps over a period of roughly 5 min. The corresponding strain-field loop for the same sample (at 0.1 Hz) is shown in Fig. 5. The sample orientation and the direction of polarizer and analyzer are the same for each image and are shown in (a) and (e), respectively.

polarizer (P) and analyzer (A) directions, the crystal is brightly birefringent as shown in Fig.6(a). No clearly defined domain walls are visible although the inhomogeneity of the birefingence pattern suggests a complicated domain structure. The crystal shows complete extinction when the crystal is rotated in one direction, $30°\pm 90°n$, where n is an integer. Such fourfold extinction is consistent with a zero-field, psuedo-orthorhombic phase.

As the field is increased, the same interference pattern is retained although the color observed is slightly shifted towards weaker birefringences [Fig. 6(b)]. Just before the field-induced phase transition a new, characteristically extinct phase begins to nucleate in one corner of the sample (c). As the field is increased over the threshold field E_T, there is near instantaneous growth of this new phase across the entire crystal (d). This high-field phase (e) shows extinction at all angles, consistent with a rhombohedral phase oriented along the $[111]_C$ direction. Upon removal of the field, the rhombohedral phase is stable until a field of around 100 V/mm; here the previous low-field phase begins to nucleate and grow back out into the sample (f). The initial nucleation of the rhombohedral phase in one corner of the sample is perhaps indicative of easier nucleation or of a lower local threshold field due to a composition gradient across the sample.

Figure 7 shows the strain-field loop for another sample of the PZN−8PT, this time electroded with gold, upon cycling to a much higher electric field >3000 V/mm. The electric-field-induced transition is still evident, although this time at a smaller field $E_T\sim 250$ V/mm. Notably, there is a difference between the threshold fields measured for the two samples. This discrepancy in E_T could be, at least partially, due to a variation in $PbTiO_3$ content. To help quantify this, the Curie temperatures (T_C) of the two samples were found by measuring permittivity upon heating to the paraelectric phase. The T_C of the gold-electroded sample was found to be around 5 °C higher than that of the ITO-electroded one which, upon comparison with the phase diagram for the PZN−xPT,[28] suggests a possible difference in $PbTiO_3$ con-

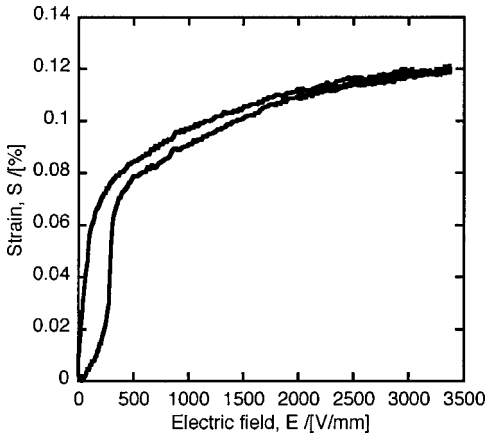

FIG. 7. Strain-field loop for a $[111]_C$-oriented sample of PZN−8PT after unipolar cycling to fields <4000 V/mm. The strain was measured at a frequency of 0.1 Hz using a fiber-optic system.

tent of up to 1%. However, this approach is not conclusive as other factors, including internal stresses,[29] can also affect the Curie temperature.

Two other possible causes for the differing threshold fields are the change in electrode material and the different surface preparations, especially since the ITO-electroded sample had been previously diamond polished and annealed. Since nucleation of the new phase is most likely to occur heterogeneously at the crystal surface,[30,31] the rough, as-cut, gold-electroded surface with many defects could facilitate the field-induced phase transition, whereas the smooth, relaxed, ITO-electroded surface with fewer imperfections would not. The effect of the electrode material and the surface condition on the electric-field-induced phase transition in these crystals, and indeed the nucleation and growth mechanism for the transition itself, would be worthy of further investigation.

After the phase transition, the loop is somewhat hysteretic probably due to the residual domain reorientation in the rhombohedral phase. However, the sample does approach an anhysteretic, monodomain (1*R*) state at higher fields >3000 V/mm, where the gradient gives an estimate of d_{33} ~70 pm/V; this is similar to the corresponding values of 110 and 125 pm/V measured for the PMN−33PT and PZN−4.5PT, respectively. It might be noted that the strain-field loops in Figs. 4 and 7 look similar. However, consideration of the scales of the two loops (at 1000 V/mm the PZN−8PT shows a strain roughly three times as large as that in the PMN−33PT) will reiterate the effect of the field-induced phase transition.

Another point of note from Figs. 5 and 7 is that the field-induced phase transition is reversible overall, i.e., the pseudo-orthorhombic phase is retained after the removal of the field. In previous work,[11] it was found that a rhombohedral phase could be stabilized in a $[111]_C$-oriented sample of PZN−8PT by poling under 500 V/mm at subzero temperatures. The results suggest that the low temperature is most important in "freezing in" the metastable rhombohedral phase.

Finally, it is interesting to speculate on the rotation path occurring during the transition. Considering the limiting polarization directions of $[101]_C$ and $[111]_C$, and comparing to work done elsewhere, it is likely that the simplest polarization rotation in the $(10\text{-}1)_C$ plane will occur, i.e., via the M_B monoclinic phase. This rotation path O-M_B-R is the reverse of that suggested by Viehland and Li for the rhombohedral to orthorhombic transition they observed in PMN−30PT.[23] However, in the case of the PZN−8PT presented here, a hysteretic strain-field loop and the mobile phase boundary observed *in situ* evidence a first-order, irreversible jump in polarization and therefore the presence of competing, metastable M_B and R states. In contrast, the loop observed by Viehland and Li was anhysteretic, suggesting a continuous rotation or a second-order-like transition. These differing rotation behaviors might not be unexpected based on the first-principles calculations of Bellaiche *et al.* There, for PZT at the MPB, a rhombohedral phase oriented along the $[001]_C$ direction transforming to a tetragonal phase and a tetragonal phase oriented along the $[111]_C$ direction transforming to a rhombohedral phase even follow different rotation paths.[16]

Furthermore, the same O-M_B rotation and discontinuous jump in strain to a rhombohedral phase have previously been predicted in the orthorhombic phase of $BaTiO_3$, by Bell, using phenomenological theory.[20] However, to confirm the O-M_B-R rotation path in PZN−8PT, *in situ* diffraction studies are needed and should be reconciled with the macroscopic strain-field loops and optical observations presented here.

IV. CONCLUSIONS

An electric-field-induced phase transition has been observed in $[111]_C$-oriented, pseudo-orthorhombic PZN−8PT by strain-field measurements and *in situ* polarized light microscopy. The transition occurs most likely via polarization rotation in the $(10\text{-}1)_C$ mirror plane of a M_B monoclinic phase, i.e., it follows the inverse of the R-M_B-O rotation path observed in the $[101]_C$-oriented PMN−30PT.[23] However, in the case presented here, the strain-field loop is hysteretic, indicating that the O-M_B-R polarization rotation is not completely reversible. The work reiterates the universality of the electric-field-induced phase transition, especially for relaxor-ferroelectric single crystals close to the morphotropic phase boundary where the rhombohedral, orthorhombic, and monoclinic phases are nearly degenerates.

ACKNOWLEDGMENTS

The authors would like to acknowledge the support of the Swiss National Science Foundation. The authors would also like to acknowledge the help of Dr. Simon Buehlmann with sputtering. The LVDT system used was built at EPFL following a design by Paul Moses from Penn State University.

[1] S.-E. E. Park and T. R. Shrout, J. Appl. Phys. **82**, 1804 (1997).
[2] S.-E. E. Park and W. Hackenberger, Curr. Opin. Solid State Mater. Sci. **6**, 11 (2002).
[3] B. Noheda, Curr. Opin. Solid State Mater. Sci. **6**, 27 (2002).
[4] Z.-G. Ye, Curr. Opin. Solid State Mater. Sci. **6**, 35 (2002).
[5] B. Noheda, Z. Zhong, D. E. Cox, G. Shirane, S.-E. Park, and P. Rehrig, Phys. Rev. B **65**, 224101 (2002).
[6] K. Ohwada, K. Hirota, P. W. Rehrig, Y. Fujii, and G. Shirane, Phys. Rev. B **67**, 094111 (2003).

[7]B. Noheda, D. E. Cox, G. Shirane, J. Gao, and Z.-G. Ye, Phys. Rev. B **66**, 054104 (2002).
[8]Y. Lu, D.-Y. Jeong, Z.-Y. Cheng, T. Shrout, and Q. M. Zhang, Appl. Phys. Lett. **80**, 1918 (2002).
[9]S. Priya, J. Ryu, L. E. Cross, K. Uchino, and D. Viehland, Ferroelectrics **274**, 121 (2002).
[10]A. A. Bokov and Z.-G. Ye, J. Appl. Phys. **95**, 6347 (2004).
[11]M. Davis, D. Damjanovic, and N. Setter, J. Appl. Phys. **96**, 2811 (2004).
[12]D. Vanderbilt and M. H. Cohen, Phys. Rev. B **63**, 094108 (2001).
[13]D. Damjanovic, M. Budimir, M. Davis, and N. Setter, Appl. Phys. Lett. **83**, 527 (2003).
[14]S. Wada, H. Kakemoto, and T. Tsurumi, Mater. Trans., JIM **45**, 178 (2004).
[15]H. Fu and R. E. Cohen, Nature (London) **403**, 281 (2000).
[16]L. Bellaiche, A. Garcia, and D. Vanderbilt, Phys. Rev. B **64**, 060103(R) (2001).
[17]D. Damjanovic, F. Brem, and N. Setter, Appl. Phys. Lett. **80**, 652 (2002).
[18]M. Budimir, D. Damjanovic, and N. Setter, J. Appl. Phys. **94**, 6753 (2003).
[19]X.-H. Du, J. Zheng, U. Belegundu, and K. Uchino, Appl. Phys. Lett. **72**, 2421 (1998).
[20]A. J. Bell, J. Appl. Phys. **89**, 3907 (2001).
[21]S.-F. Liu, S.-E. Park, T. R. Shrout, and L. E. Cross, J. Appl. Phys. **85**, 2810 (1999).
[22]W. Ren, S.-F. Liu, and B. K. Mukherjee, Appl. Phys. Lett. **80**, 3174 (2002).
[23]D. Viehland and J. F. Li, J. Appl. Phys. **92**, 7690 (2002).
[24]M. Daglish, Integr. Ferroelectr. **22**, 473 (1998).
[25]M. K. Durbin, E. W. Jacobs, and J. C. Hicks, Appl. Phys. Lett. **74**, 2848 (1999).
[26]R. Zhang, B. Jiang, and W. Cao, Appl. Phys. Lett. **82**, 787 (2003).
[27]C.-S. Tu, I.-C. Shih, V. H. Schmidt, and R. Chien, Appl. Phys. Lett. **83**, 1833 (2003).
[28]M. K. Durbin, J. C. Hicks, S.-E. Park, and T. R. Shrout, J. Appl. Phys. **87**, 8159 (2000).
[29]G. A. Rossetti, L. E. Cross, and K. Kushida, Appl. Phys. Lett. **59**, 2524 (1991).
[30]W. Cao, S. Tavener, and S. Xie, J. Appl. Phys. **86**, 5739 (1999).
[31]A. K. Tagantsev, I. Stolichnov, E. L. Colla, and N. Setter, J. Appl. Phys. **90**, 1387 (2001).